

Integrated stratigraphy of the Ypresian–Lutetian transition in northern Tunisia: Correlation and paleoenvironmental reconstruction



Narjess Karoui-Yaakoub^{a,b}, Moufida Ben M'Barek-Jemaï^a, Moncef Saïd Mtimet^a, Eustoquio Molina^{c,*}

^aUniversité de Carthage, Faculté des Sciences de Bizerte, Département des Sciences de la Terre, Jarzouna, Bizerte 7021, Tunisia

^bUnité de recherche: Pétrologie sédimentaire et cristalline, Université de Tunis El Manar, Tunisia

^cDepartamento de Ciencias de la Tierra & IUCA, Universidad de Zaragoza, E-50009 Zaragoza, Spain

ARTICLE INFO

Article history:

Received 26 March 2015

Received in revised form 30 June 2015

Accepted 1 July 2015

Available online 2 July 2015

Keywords:

Foraminifera

Clay mineralogy

Ypresian/Lutetian boundary

Chronostratigraphy

Paleoenvironment

Tunisia

ABSTRACT

Micropaleontological, mineralogical and geochemical data of the Ypresian–Lutetian transition at the Sejen section, Tunisia, allowed us to trace a precise correlation with the Global Stratotype Section and Point for the Ypresian/Lutetian boundary recently defined at Gorrondatxe, Spain. The planktic foraminifera assemblages are diversified and enable the biozones of *Acarinina pentacamerata* (E6), *Acarinina cuneicamerata* (E7a), *Turborotalia frontosa* (E7b), *Guembelitrioides nuttalli* (E8) and *Globigerinatheka kugleri/Morozovella aragonensis* (E9) to be identified, revealing a hiatus across the E8/E9 boundary. Comparison with the boundary stratotype indicates that the Ypresian/Lutetian boundary in the Sejen section is located near the base of the E7b zone, just above the first appearance of the species *T. frontosa*. In the Sejen section, there are several events identical to those recorded in the boundary stratotype at the Gorrondatxe section. In the middle of this interval, the species diversity of planktic foraminifera is the first to decline, followed by that of the benthic foraminifera in the two sections. Furthermore, taxa with calcareous test peter out while those with agglutinated test reach their peak. There is a marked fall in carbonates in the two sections; while also variations in clay minerals, smectite and kaolinite are very abundant. In the Sejen section, smectite is the dominant mineral and silica reached its peak. All these data indicate that in northern Tunisia at the Ypresian–Lutetian transition, the marine environment was deep and bathyal, with low energy, oxygenated and characterized by a warm tropical to subtropical climate. Consequently, the Sejen section may be a suitable section to be defined as auxiliary section (=hypostratotype).

© 2015 Elsevier Ltd. All rights reserved.

1. Introduction

The International Subcommission on Paleogene Stratigraphy (ISPS) set up a working group to select the Global Stratotype Section and Point (GSSP) for the base of the Lutetian Stage. The stratotype of the Ypresian/Lutetian (Y/L) boundary should be defined at a level stratigraphically close to the base of the classic Lutetian Stage, which is the lowest stage of the middle Eocene (Jenkins and Luterbacher, 1992). Since 1992, the most active members of the working group have visited and sampled several sections in Italy, Israel, Tunisia, Morocco, Mexico, Argentina and several regions in Spain, in order to find a suitable candidate to define the GSSP. Most of the sections found are not suitable as they present stratigraphic hiatuses, facies that are inappropriate for correlation, tectonic complications and other problems (Gonzalo

et al., 2001; Payros et al., 2006), but eventually a suitable candidate was found and the GSSP was defined at the Gorrondatxe section, Spain (Molina et al., 2011).

According to Luterbacher et al. (2004) and Steurbaut (2006), the Ypresian Stage was introduced by Dumont in 1849 to include clay and sandy facies strata located between the continental to margino-littoral Landenian deposits and the marine Brussels Sands, in Belgium. The Ypresian Stage was defined by the associations of calcareous nannofossils (Martini, 1971; Vandenberghe et al., 1998; Steurbaut, 1988, 2006). The Lutetian Stage stratotype, which is about 50 km to the north of Paris, was selected by Blondeau (1981). It contains large foraminifera, palynomorphs and calcareous nannofossils. According to Aubry (1983, 1986), the base of the Lutetian stage is located within the calcareous nanno-plankton zone NP14 of Martini (1971), near the boundary of zones CP12a/CP12b of Okada and Bukry (1980); the stage extends to NP15 and the lower part of NP16. Regarding magnetostratigraphy, the basal deposits of the Lutetian stage stratotype have been correlated

* Corresponding author.

E-mail address: emolina@unizar.es (E. Molina).

with the Earnley Formation of England, whose base corresponds to the Chron C21r (Ali and Hailwood, 1995).

Regarding planktic foraminiferal biostratigraphy, Hooyberghs (1992) studied two sections of the base of the Brussels Formation in the Brussels-Leuven region, which allowed him to identify planktic foraminifera attributable to the P9 Zone (=Acarinina aspensis) of Blow (1979) in one of the sections, and to the P10 Zone (=Turborotalia frontosa) in the other section. Micropaleontologists have proposed the first appearance of *Hantkenina nuttalli* to define the Y/L boundary (Toumarkine and Luterbacher, 1985; Berggren et al., 1995); consequently, this event was used to place the Y/L boundary on the Agost section (Gonzalvo and Molina, 1998; Molina et al., 2000; Larrasoña et al., 2008; Ortiz et al., 2008), the Fortuna section (Molina et al., 2006; Ortiz and Thomas, 2006) and the Gorrondatxe section (Orue-Etxebarria et al., 2006; Bernaola et al., 2006; Payros et al., 2006, 2007, 2009a, 2009b). Nevertheless, the ISPS working group demonstrated that the first appearance of *H. nuttalli* is more recent than the base of the classic Lutetian Basin of Paris (Orue-Etxebarria et al., 2009).

After intensive work, the ISPS working group defined the GSSP for the base of the Lutetian Stage at the Gorrondatxe section, near Bilbao, Spain (Molina et al., 2011). The micropaleontological event that corresponds most closely to the base of the historical Lutetian Stage was chosen as the marker for the GSSP. This seemed to be the lowest occurrence of the calcareous nannofossil *Blackites inflatus* (CP12a/b boundary), just above the lowest occurrence of the planktic foraminifera *T. frontosa*, which is in the middle of polarity Chron C21r. This event coincides with a dark marly level, which has been interpreted as the maximum flooding surface of a depositional sequence that may be global in extent (Bernaola et al., 2006; Payros et al., 2007, 2009a,b; Orue-Etxebarria et al., 2009; Rodríguez-Tovar et al., 2010; Ortiz et al., 2011; Molina et al., 2011; Payros et al., 2012).

The aim of this study is to identify the Y/L boundary at the Sejnen section in northern Tunisia, to characterize its environment of deposition and to correlate it with the GSSP of the Y/L defined at the Gorrondatxe section in Spain. Here, we present an integrated stratigraphy of foraminifera, clay minerals and geochemistry, taking into account our previous studies in Spain (Molina et al., 2011), in order to find suitable sections which could serve to propose candidates as auxiliary sections or hypostratotypes.

2. Geographical and geological setting

The section is located in northern Tunisia, in the northern Alpine region with outcrops sediments spanning from the Triassic to the Oligocene, deposited in a normal stratigraphic succession (Fig. 1). Near the Triassic diapiric structure, the outcrops are dislocated by an EW fault system. The Sejnen section is located in the vicinity of the isoclinal folds to the north of the geological map of Hedhil No. 11, scale 1/50,000 at the geographical coordinates: 37°3'55,81" N, 9°21'31,20" E. The section is easily accessible by the main road GP7 from the El Aouena village to Sejnen town and it is placed on the eastern side of a narrow track taken approximately 2 km after the intersection of El Aouena.

The Y-L transition sediments are included in the syncline of the Sidi Abdallah Ben Said region toward the south of the Sejnen town, specifically the gray marls of Souar Formation. These marls are well exposed along the road linking the towns of Mateur and Sejnen (Fig. 1). The total thickness of the section is about 125 m. It is composed of hemimetric calcareous beds, gray-beige in color, which are overlain by gray marls rich in iron oxides and sometimes characterized by a crumbly appearance. These marls sometimes become compact and rich in carbonates at the base and the top.

3. Materials and methods

On the field, twenty marl samples were collected across the Y/L boundary to study the planktic and the small benthic foraminifera, the clay minerals and the chemical elements. In the laboratory, the marls samples were previously dried in a stove at a temperature below 50 °C. Of this dry material, 300 g were soaked in the tap water and H₂O₂ for 2–3 days. The washing was conducted on an AFNOR sieves, column whose meshes were successively 315 µm, 100 µm and 63 µm. When necessary the tests were cleaned using an ultrasound device. The residues obtained were dried in an oven at less than 50 °C and then sorted under a binocular microscope in order to study the foraminifera. The photographic images were made using the scanning electron microscope (SEM) at the laboratory of the Tunisian Enterprise of Petroleum Activities (ETAP).

The determination of the CaCO₃ content of the clays was performed by the Bernard method. This test measures the volume of CO₂ released during the decomposition of 0.5 g of finely ground clay and dried with 10 ml of hydrochloric acid (10% HCl). Mineralogical analyses were performed by X-ray diffraction on the total rock and on the clay fraction <2 µm. Previously crumbled clay particles, freed from coarse material through a sieve of 63 microns, underwent decarbonation, elimination of organic matter and deflocculation by at least 3 cycles of centrifugation for 10 min at 2500 rev/min until obtaining a pellet. The cloudy supernatant then sedimented freely on smooth glass slides and was analyzed by diffractometry in 3 distinct states: normal, glycolated and baked at 550° (Chamley, 1971).

Chemical analyses of the clays were performed according the method of spectrochemical analysis by X-ray fluorescence, which is based on characteristics of the radiation emitted by the chemical elements of a sample when excited by a suitable source. The direct excitation by electron bombardment is generally used in electron microscopes whereas radioisotope sources and the protons generators are commonly associated with the analysis technique by dispersive energy. This method required the preparation of clay pellets.

4. Results

4.1. Description of the benthic and planktic foraminifera assemblages

Observation under a binocular microscope of residues from different samples from the basal marls, approximately 72 m thick (Sj.1 to Sj.11) revealed an abundant foraminifera association, which was diversified and well preserved. The planktic foraminifera species belong mainly to the genera *Morozovella*, *Acarinina*, *Chiloguembelina*, *Pseudohastigerina*, *Subbotina*, *Turborotalia*, *Globigerinatheka*, *Pseudoglobigerinella* and *Hantkenina* (Fig. 2, Pl. 1). Sometimes tests are filled, apertures obscured and tests abraded at their margins. Benthic foraminifera are represented by the genera *Gyroidinoides*, *Cibicidoides*, *Eponides*, *Anomalinooides*, *Bulimina*, *Dorothia*, *Dentalina*, *Loxostomoides*, *Spiroplectamina*, *Vaginulinopsis*, *Stilostomella*, *Nuttallides*, *Subreophax* and *Nodosaria* (Fig. 3).

These levels are overlain by 10 m of gray marls with abundant microfauna, diversified and well preserved, wherein the species *Guembelitrioides nuttalli* appears near the top at the Sj.12 sample. Above this, there are 30 m of gray marls richer in carbonates where new species of planktic foraminifera are observed from the sample Sj.14, including the marker *Globigerinatheka kugleri*.

4.2. Biodiversity of benthic and planktic foraminifera

The systematic study of the foraminifera shows that they are numerous and diversified (Figs. 2 and 4, Table 1). In sample Sj.3, the planktic foraminifera were numerous: 23 species, 7 belonging

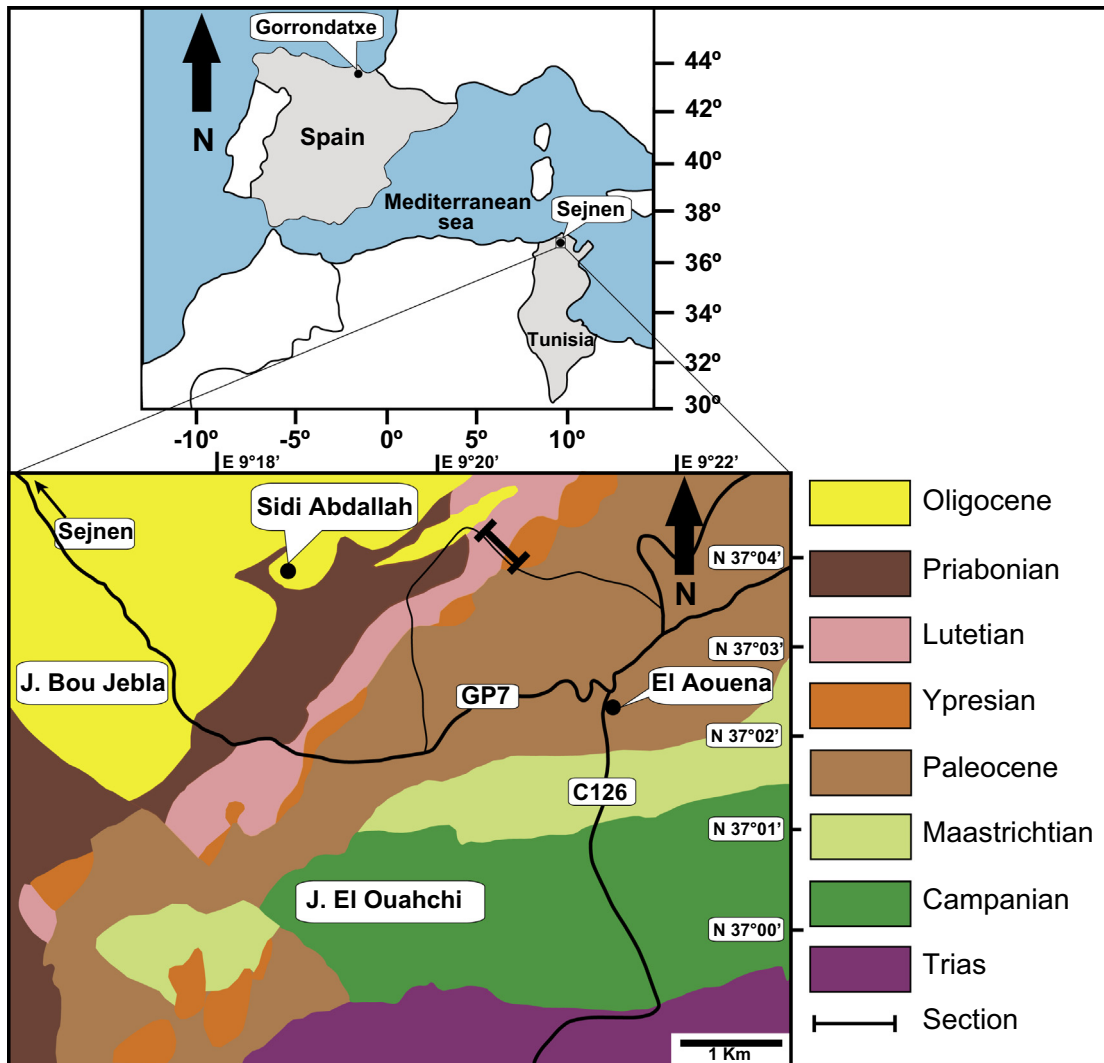


Fig. 1. Geographical and geological location of the Sejnen section.

to the genera *Morozovella*, 8 *Acarinina*, 5 *Subbotina*, 1 *Chiloguembelina* and 2 *Pseudohastigerina*. At 47 meters above the base, at the level of Sj.9 the species belonging to the genera *Morozovella* and *Acarinina* are dominant. In the sample Sj.14, about 114 m above, planktic foraminifera again become numerous and diversified, reaching a maximum of 30 taxa; in addition, the spherical forms (Globigeriniforms) predominate over the keeled forms (16 of 12).

Benthic foraminifera show greater species diversity than planktic and infaunal species clearly predominating over epifaunal species (Figs. 3 and 4, Table 1). In the sample interval Sj.1–Sj.7, the number of benthic foraminifera species clearly exceeds that of planktic foraminifera. It is almost double in the sample Sj.3 where there are 45 taxa of benthic foraminifera, the maximum amount and the number of planktic taxa is equal to 23. In the same sample, benthic foraminifera comprise 33 infaunal species for only 12 epifaunal. In Sj.7–Sj.11 interval, species richness of planktic foraminifera bottoms out in the Sj.9 sample at 12 species, while benthic foraminifera remain abundant and nearly triple in number (37 species). In this same sample Sj.9, agglutinated forms reach their maximum (13 taxa). In Sj.11, the number of benthic foraminifera falls to 23 taxa of which 16 are infaunal species and 7 are epifaunal. This decline in benthic foraminifera continues throughout the Sj.11–Sj.15 interval where they reach their minimum, 21

taxa in Sj.15, which is a consistent predominance of infaunal species (14 infaunal and 7 epifaunal). It is remarkable that in this interval the state of preservation of foraminifera has been much degraded: tests become fragmented, ferruginized and dissolved.

However, for the planktic foraminifera the percentages are reversed at the last samples (Sj.14 and Sj.15). Indeed, the number of planktic foraminifera progressively overtakes that of the benthic foraminifera; moreover, from Sj.11, the conditions change and the number of planktic foraminifera increases (15 species) then peak at 30 in sample Sj.14. Therefore, in this interval the planktic foraminifera thrive, proliferate and diversify after a crisis whereas the benthic foraminifera maintain an average value of 22 species. However, this value is less relevant than the initial value (Fig. 4; Table 1). The ratio PLF/PLF + BF roughly follows the shape of the curve of planktic foraminifera and indicates an index of oceanity (see Bellier et al., 2010; Fig. 11), which reaches a minimum value of 24.48% in Sj.9. The maximum value of this indicator is 56.6% in Sj.14. In the interval Sj.7–Sj.9 agglutinated forms are very abundant and reach their maximum values (Fig. 4; Table 1). The association of benthic foraminifera is a mixture of Midway and Velasco types (Berggren and Aubert, 1975). The main Midway type species are *Cibicidoides allenii*, *C. succedens*, *Anomalinoides acuta*, *A. midwayensis*, *Lenticulina midwayensis* and *Anomalina dani*. Meanwhile the main Velasco type species are: *Nuttalides truempyi*,

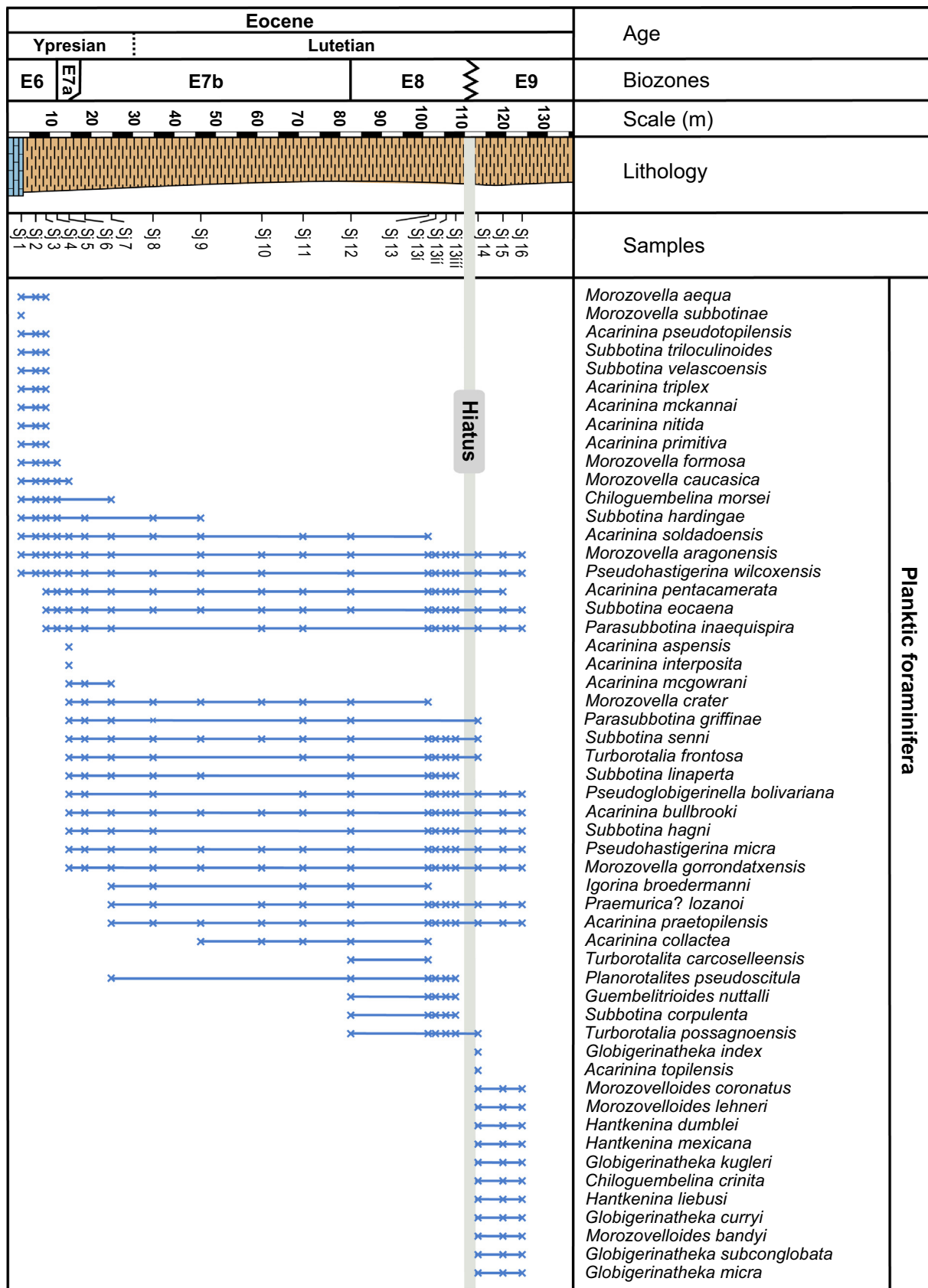


Fig. 2. Vertical distribution of planktic foraminifera at the Y/L boundary in the Sejnen section.

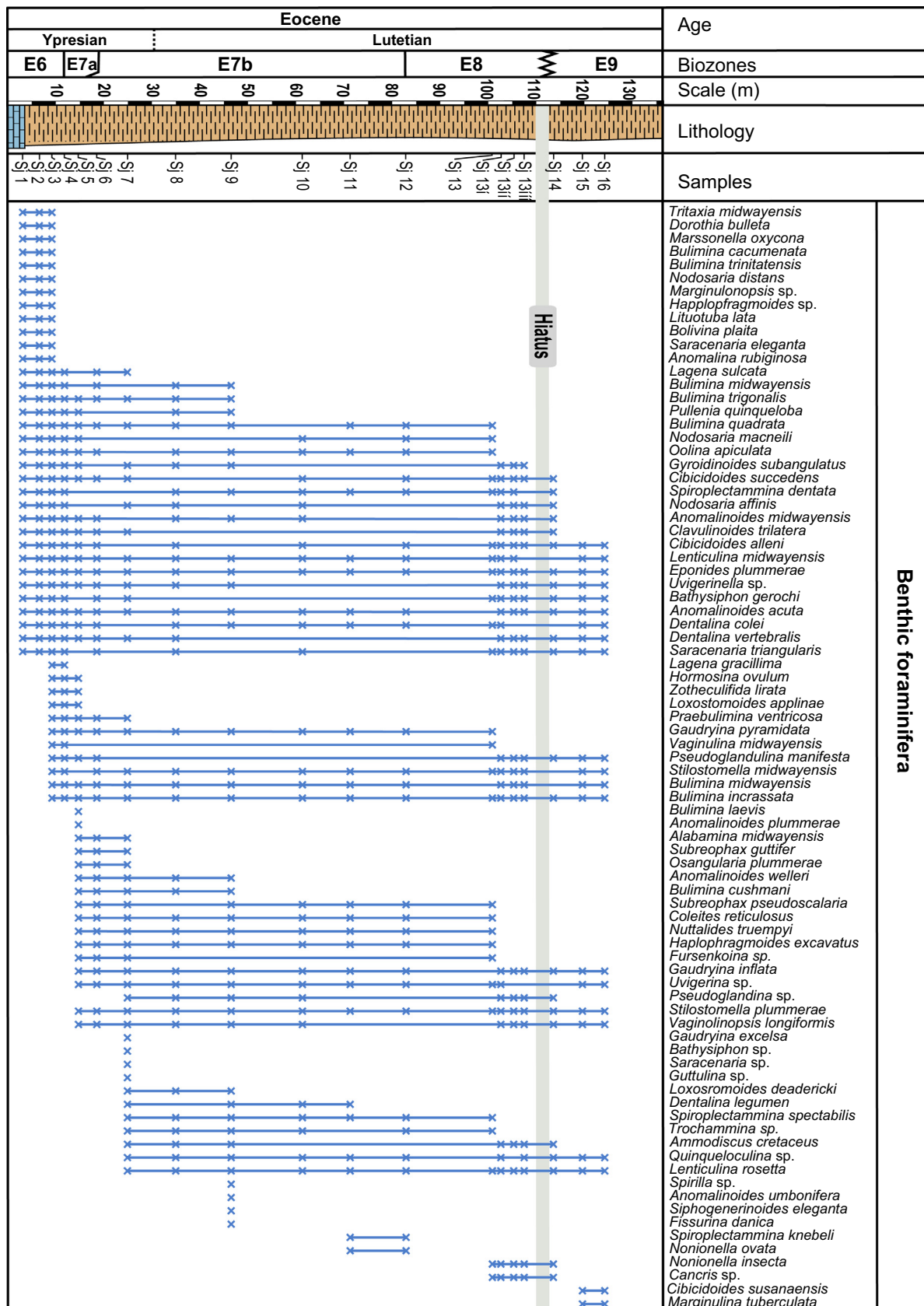


Fig. 3. Vertical distribution of benthic foraminifera at the Y/L boundary in the Sejen section.

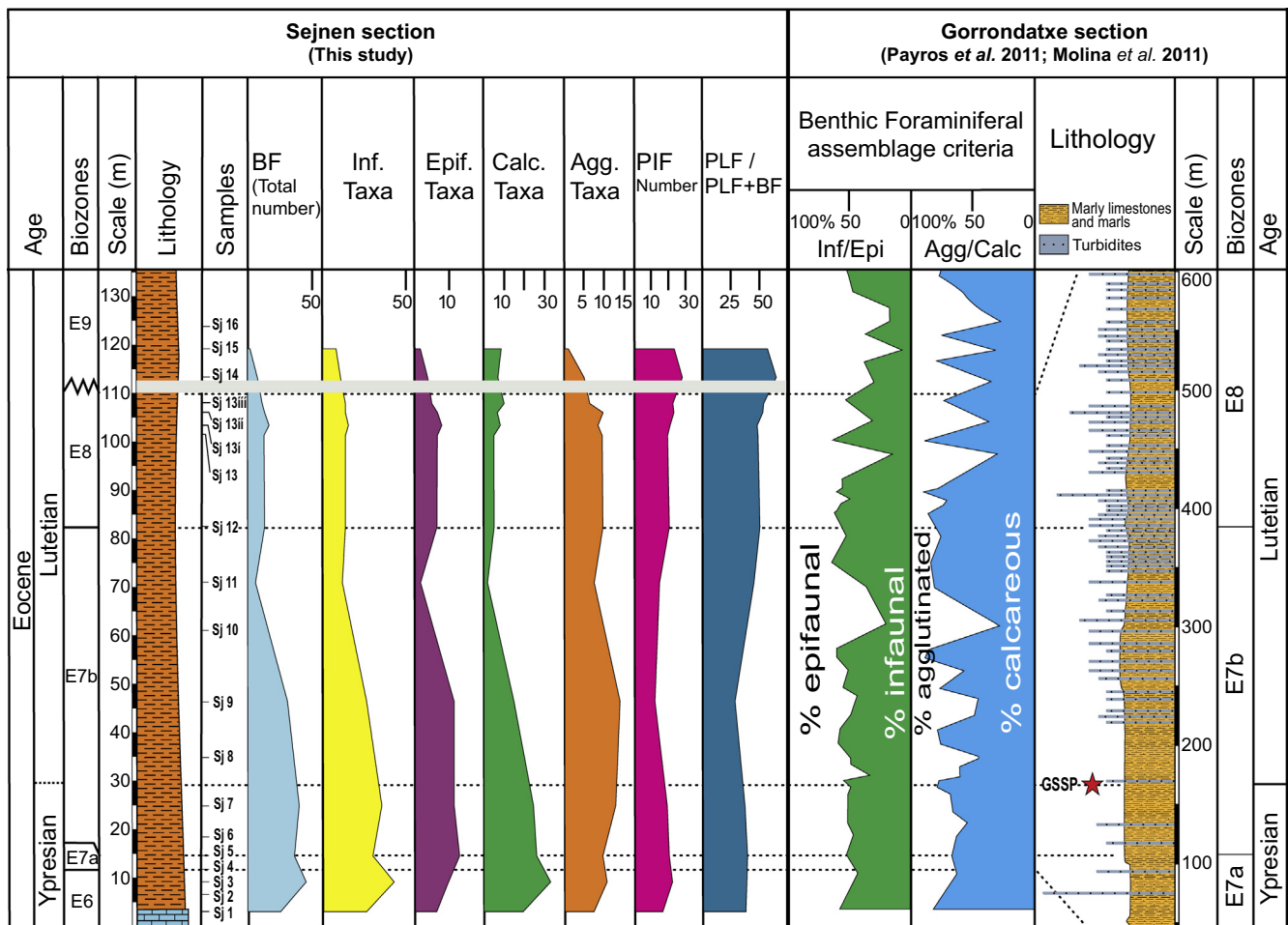


Fig. 4. Variation in the species richness of benthic and planktic foraminifera and correlation with the Gorrondatxe stratotype.

Table 1

Variation in the number of planktic and benthic foraminifera and in the ratio of planktic to the sum of planktic and benthic foraminifera.

Scale (m)	Sample	Endobenthonic foraminifera	Epibenthonic foraminifera	Calcareous foraminifera	Agglutinated foraminifera	Benthic	Planktic	PLF/PLF + BF%
3	Sj1	24	10	27	7	34	17	33.33
9	Sj3	33	12	35	10	45	23	33.82
15	Sj5	26	14	31	9	40	21	34.42
25	Sj7	29	13	30	12	42	20	32.25
47	Sj9	24	13	24	13	37	12	24.48
72	Sj11	16	7	16	7	23	15	39.47
83	Sj12	17	10	18	9	27	21	43.75
102	Sj13	17	10	18	9	27	20	42.55
104	Sj13'	18	11	20	9	29	21	42.00
107	Sj13''	17	10	18	9	27	24	47.05
109	Sj13'''	17	9	20	6	26	23	46.94
114	Sj14	15	8	19	4	23	30	56.60
120	Sj15	14	7	20	1	21	23	52.27

Anomalinoides rubiginosa, *Gyroidinoides subangulatus* and *Gaudryina pyramidata*.

4.3. Evolution of clay assemblages and chemical elements content

Mineralogical and chemical analysis of the clays indicates the abundance of kaolinite, illite and smectite with a high crystallinity. In Fig. 5 and Table 2, we can see that the content of clay minerals varies throughout the Y-L interval. In the sample interval Sj.3–Sj.7, smectite and illite have relevant contents with a peak of 51.80% for the smectite in Sj.5 and 24.87% for the illite, respectively. Kaolinite

is very abundant with a maximum content of 64.8% in Sj.3 and a minimum of 23.31% in Sj.5. The kaolinite/smectite (K/S) ratio is low with a rate which varies from 2.00% to 0.89%. Therefore, at the base of the section, smectite and illite are less abundant and have lower contents than the kaolinite. In the Sj.8–Sj.13 interval, kaolinite is present with a content which varies from a maximum of 18.80% and a minimum of 8.14%. Smectite is very abundant, almost constant with a maximum of 86.93% in Sj.10, but we note that it falls slightly (to 57%) at Sj.12. In the same sample Sj.12, we note a small peak at 22% of kaolinite between two lower values. Illite behaves in two distinct ways: it is very weak in the first half

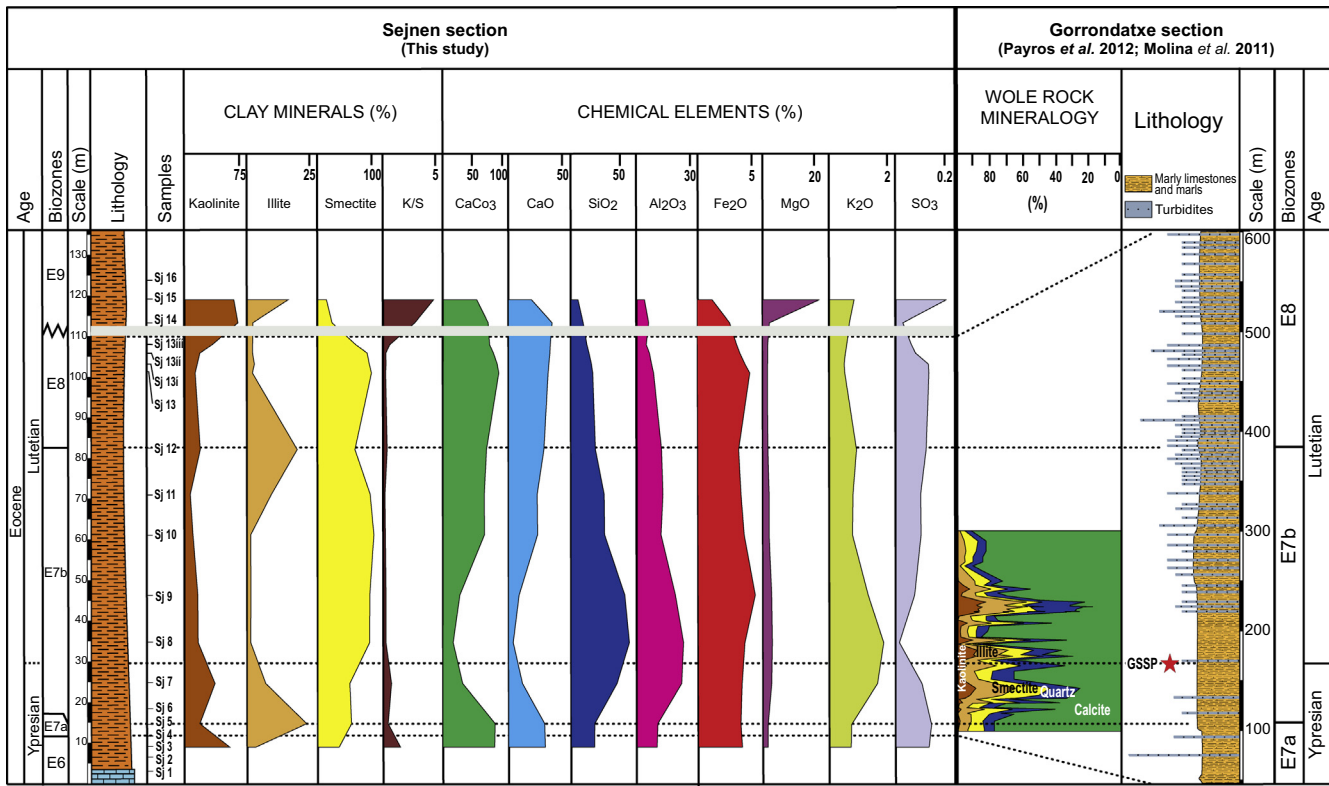


Fig. 5. Richness in clay mineral and chemical elements and correlation with the Gorrondatxe stratotype.

Table 2
Table of contents of clay minerals.

Scale (m)	Sample	Kaolinite %	Smectite %	Illite %	Kaolinite/ smectite
9	Sj3	64.80	32.00	3.20	2.00
15	Sj5	23.31	51.80	24.87	0.45
25	Sj7	43.54	48.98	7.47	0.89
35	Sj8	18.80	80.20	1.00	0.23
47	Sj9	18.55	80.53	1.13	0.23
62	Sj10	11.96	86.93	1.10	0.14
72	Sj11	8.14	82.00	9.84	0.10
83	Sj12	22.00	57.00	21.00	0.38
102	Sj13	14.96	83.26	1.76	0.18
104	Sj13'	17.53	79.86	2.59	0.21
107	Sj13''	21.24	76.93	1.83	0.21
109	Sj13'''	39.43	58.66	1.87	0.67
114	Sj14	76.97	21.03	2.00	3.66
120	Sj15	70.99	12.00	16.98	5.92

of the interval, from Sj.8 to Sj.10 but then increases and reaches a sharp peak of 21% in Sj.12, before falling back in Sj.13. The K/S ratio decreases in this interval. This abundance of smectite is also recorded in the Gorrondatxe section (Fig. 5). In the interval Sj.13–Sj.15, kaolinite becomes more abundant with a maximum content of approximately 77% at Sj.14, whereas smectite rate decreases to a low of 21.03%; therefore, the K/S ratio increases to 3.66%. The illite content remains lower with a first peak of 2% at Sj.14 (Table 2). This has already been noted by Jamoussi et al. (2003) in their studies on the basins of the Tunisian margin in the upper Cretaceous-Lutetian interval.

In the sample interval Sj.3–Sj.10, the rates of carbonate (CaO and CaCO₃) and SO₃, decrease and reach the minimum at the sample Sj.8. Indeed in this sample, the rate of CaCO₃ falls to 11.88%, with 3.99% for CaO and 0.046% for SO₃. In contrast, the silica (SiO₂) content rises to a peak of 52.597%. The contents of Al₂O₃ (21.59%), Fe₂O (4.067%), MgO (2.784%) and K₂O (1.83%) also increase (Fig. 5;

Table 3). In the Sj.11–Sj.14 interval, carbonate rates increase with a maximum occurring in sample Sj.13 (CaCO₃ = 66.22%) and also the SO₃ rate (0.14%). However, in the same interval, the contents of SiO₂, Al₂O₃ and K₂O decrease albeit, remaining relatively high, while the Fe₂O content remains almost constant. In the last sample Sj.15, the contents of all elements decrease except for the MgO and SO₃, which show an abnormal increase (Fig. 5; Table 3).

5. Discussion

5.1. Planktic foraminifera biostratigraphy

At the Sejnen section, based on planktic foraminifera we identified the following biozones of Wade et al. (2011): the E6 Zone, whose base is not represented in the Sejnen section and whose upper limit is the last appearance of the species *Morozovella formosa*, which coincides with the first appearance of *Acarinina cuneicamerata*; the E7a Zone or *A. cuneicamerata* Zone, whose top is defined by the first appearance of the species *T. frontosa* (which first appears in Sj.5, 15 m from the base of the section); the E7b Zone or *T. frontosa* Zone, whose base is defined by the first appearance of the species *T. frontosa* and the top by the first appearance of the species *G. nuttalli* at the sample Sj.12 located at 83 m from the base; the E8 Zone or *G. nuttalli* Zone, whose base is defined by the first appearance of the species *G. nuttalli*; its top was not found because there is the association of both *G. kugleri* and *Morozovella aragonensis* species in the sample Sj.14 located about 114 m from the base, so the upper part of the zone E8 is missing. With regard to the E9 Zone or *G. kugleri/M. aragonensis* Zone, the base of this zone was not found suggesting a hiatus in the boundary E8/E9 highlighted by the simultaneous existence, from the base, of the species markers, *M. aragonensis* and *G. kugleri* (Pearson et al., 2006; Wade et al., 2011; Vandenberghe et al., 2012) (see Plate 1).

Table 3

Table of contents of chemical elements.

Scale (m)	Sample	CaO %	CaCO ₃ %	SiO ₂ %	Al ₂ O ₃ %	Fe ₂ O %	MgO %	K ₂ O %	SO ₃ %
9	Sj3	31.01	61.6	22.918	9.128	3.92	1.323	0.738	0.15
15	Sj5	30.54	62.04	23.38	9.596	3.789	1.365	0.778	0.16
5	Sj7	11.66	23.54	42.275	20.701	3.903	2.466	1.659	0.126
35	Sj8	3.99	11.88	52.597	21.59	4.067	2.784	1.83	0.046
47	Sj9	8.91	19.58	48.656	18.038	4.943	2.521	1.31	0.1
62	Sj10	24.47	49.28	31.933	11.07	4.05	1.677	0.818	0.123
72	Sj11	24.08	48.84	31.276	11.94	3.775	1.647	0.821	0.12
83	Sj12	29.79	50.86	24.143	11.348	3.612	1.228	0.926	0.14
102	Sj13	33.34	66.22	21.345	7.533	4.5	1.029	0.547	0.149
104	Sj13'	33.96	64.33	20.56	6.89	4.1	1.037	0.534	0.148
107	Sj13''	34.86	59.88	18.23	5.54	3.78	1.093	0.586	0.102
109	Sj13'''	35.23	55.32	16.54	4.12	3.53	1.21	0.61	0.089
114	Sj14	36.62	53.66	13.476	5.109	2.874	1.553	0.72	0.06
120	Sj15	19.211	40.44	8.95	3.178	1.445	18.877	0.868	0.21

We correlated the planktic foraminiferal biozonations of Berggren et al. (1995), Molina et al. (2011) and Wade et al. (2011) (Fig. 6) and compared the present findings with those of Pearson et al. (2006), Bernaola et al. (2006), Payros et al. (2009a, 2009b), and Vandenberghe et al. (2012). The Y/L boundary, defined at the first appearance of the nannoplankton *B. inflatus*, seems to be near the base of E7b Zone. In the upper part of the Sejnén section, we identified a hiatus in the biostratigraphic interval covering the boundary between biozones E8 and E9. This hiatus is probably of tectonic origin, due to compression that occurred during the Eocene (Ben Ayed, 1986; El Ghali et al., 2003; Gély and Sztrákos, 2000). In central Tunisia, Ben Ismail (1994), Ben Ismail-Latrache and Bobier (1996) were able to detect the Y/L boundary and highlight the *A. pentamerata* Zone (P9) of the upper Ypresian and the *H. nuttali* Zone (P10) of the early Lutetian. Salaj (1980) described several sections in the regions of Enfidha and around Kef, where he recognized the *Globorotalia palmerae* zone, which is equivalent to the *A. pentamerata* Zone of the upper Ypresian and the *H. nuttali* Subzone of the early Lutetian.

5.2. Paleoenvironmental reconstruction

Regarding the planktic foraminifera, the Sejnén section revealed events similar to those of the boundary stratotype defined at the Gorrondatxe section. The planktic foraminifera were numerous with a large dominance of tropical species. The species richness of planktic foraminifera decreases by about 50% throughout the entire Sj.5–Sj.11 interval and in the middle of the E7b Zone (sample Sj.9). A similar drop in the planktic foraminifera was observed in the Gorrondatxe section at the top of the Chron C21r of the Y/L interval where the percentage of planktic foraminifera also decreases by 50% (Payros et al., 2012). At the top of the section, at the base of the E9 Zone (Sj.14), planktic foraminifera proliferate and thrive after the crisis, also the diversity decreases and cold seawater forms become slightly dominant. The statistic on planktic foraminifera indicates that at the Y/L boundary the climate was rather warm and then cooled somewhat at the base of Lutetian. The index of oceanity reflects a lowest marine level in sample in the middle of the E7b Zone (sample Sj.9), whereas an increase in the sea level was reached in the base of the E9 Zone (sample Sj.14). This is probably due to the sea level rise and therefore the transgression of the Eocene, happening in conjunction with the compressive movements that occurred in the same period (Ben Ayed, 1986; El Ghali et al., 2003).

Regarding the small benthic foraminifera, they are highly diversified in the Y–L interval. Faunal indexes used in paleoenvironmental reconstruction are the species richness of benthic foraminifera, the number of infaunal and epifaunal species (mainly following Corliss, 1985; Jones and Charnock, 1985; Corliss and Chen, 1988;

Kaminski and Gradstein, 2005), the relative abundance of agglutinated and calcareous foraminifera and the ratio PLF/PLF + BF. In all the samples studied, infaunal foraminifera (mainly comprising by infaunal deeper forms with small tests, flattened and tapered) clearly dominate epifaunal foraminifera. The reduction in the benthic foraminifera in the top of the E7b Zone (sample Sj.11) could be equivalent to that reported in the Gorrondatxe section at the Chron C21n (Ortiz et al., 2008, 2011 (Fig. 5), Molina et al., 2011). Therefore compared with the Gorrondatxe section, the drop in benthic foraminifera is placed above the Y/L boundary. At the base of the E9 Zone (Sj.14–Sj.15 interval) the ratio is reversed and the planktic foraminifera clearly predominate over benthic foraminifera. At the base of the E7b Zone (Sj.7–Sj.9 interval), benthic foraminifera with agglutinated tests reach their maximum while those with calcareous tests decrease. However, the foraminifera test preservation is much deteriorated. The association of benthic foraminifera indicates the coexistence of the Midway and Velasco types (Speijer, 1994; Valchev, 2007; Stassen et al., 2012; Holbourn et al., 2013). The richness and dominance of the infaunal foraminifera indicate that in the north of Tunisia, at the Y/L boundary, the environment was bathyal, fairly quiet and sometimes became more oxygenated. The lowest oxygen content of bottom water is probably at the base of the E7b Zone (Sj.7–Sj.9 interval), where the benthic foraminifera with agglutinated tests, reach their maximum (Corliss, 1985; Jones and Charnock, 1985; Corliss and Chen, 1988; Kaminski et al., 1995; Kaminski and Gradstein, 2005; Boscolo-Galazzo et al., 2013). Indeed, in paleogeographical terms, the Sejnén section is located in the deep part of the northern Tunisian basin (Ben Ayed, 1986).

Regarding clay minerals, at the base of the section, the smectite and illite are less abundant and are lower in content than the kaolinite. In the E7b and E8 Zones (Sj.8–Sj.13 interval), the smectite content is very high and almost constant with a maximum equal of 86.93% in Sj.10 sample corresponding to the top of the E7b Zone, but we find a slight drop at Sj.12 precisely at the limit between E7b/E8, where we find a remarkably sharp spike in kaolinite of 22%. However, in the Gorrondatxe section, clay minerals rates decrease in this interval (Payros et al., 2012). The abundance of smectite indicates a subtropical to tropical origin where the rainfall was very low and the landforms were low; it would also indicate a high marine sea level and therefore a marine transgression (Robert and Kennett, 1992; Jamoussi et al., 2003). Therefore, the abundance of smectite combined with the richness in kaolinite and in well-crystallized illite in the Sejnén section, indicate that at the Y/L boundary the sedimentation coincided with a high marine level as pointed in Chamley et al. (1990). In the samples Sj.13–Sj.15, taken from the E8/E9 interval, kaolinite becomes more abundant with a maximum content equal of approximately 77%, in the Sj.14 sample, whereas the smectite content decreases

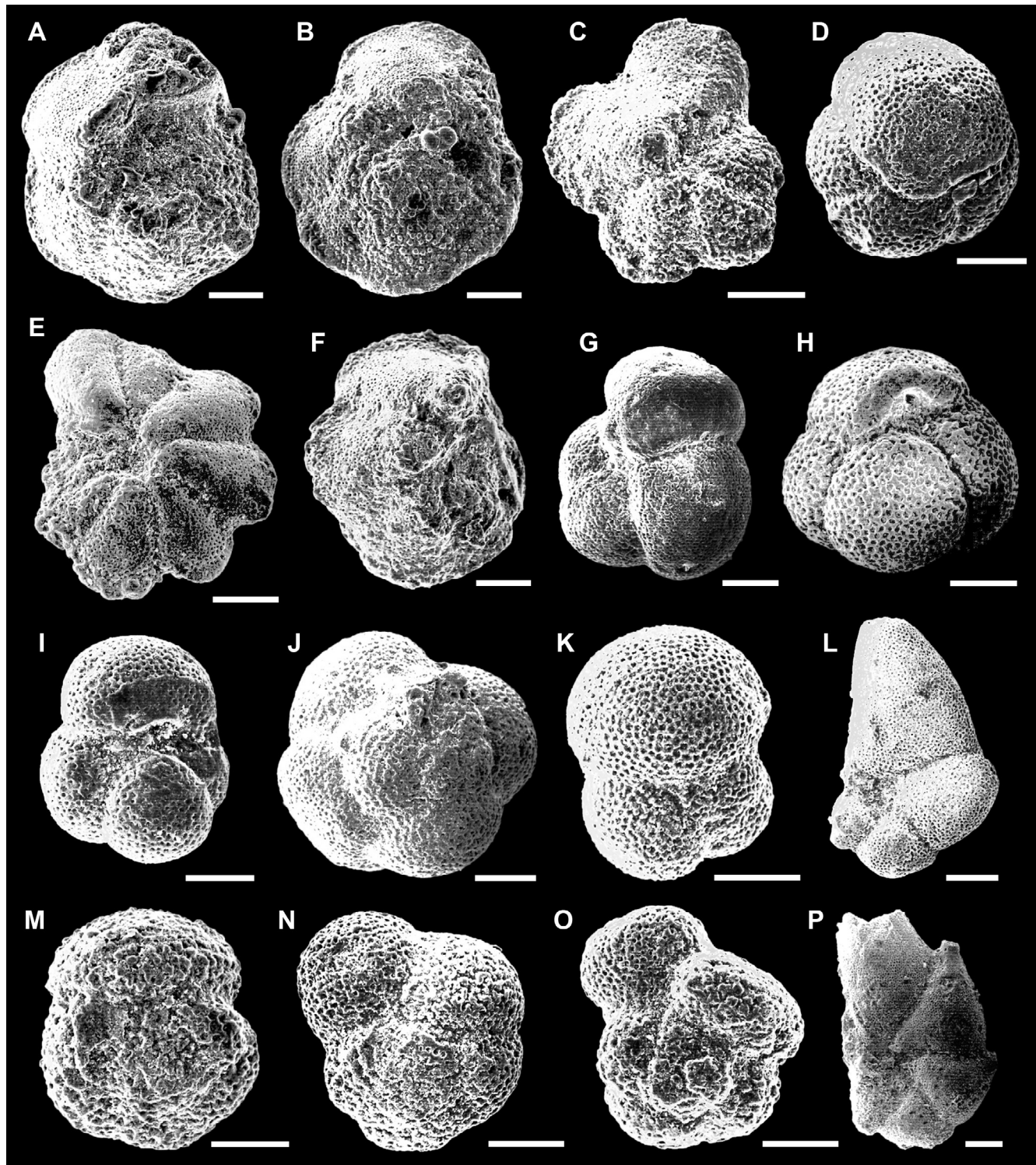


Plate 1. Planktic foraminifera from the Sejen section. A: *Morozovella caucasica*. Umbilical view. Zone E6, sample Sj.3. B: *Morozovella aragonensis*. Spiral view. Zone E7b, sample Sj.7. C: *Morozovella formosa*. Umbilical view. Zone E6, sample Sj.3. D: *Globigerinatheka* aff. *curvy*. Umbilical view. Zone E9, sample Sj.14. E: *Morozovella lehneri*. Umbilical view. Zone E9, sample Sj.14. F: *Morozovella gorrondatxensis*. Umbilical view. Zone E7b, sample Sj.8. G: *Turborotalia* sp. Umbilical view. Zone E8, sample Sj.10. H: *Globigerinatheka subconglobata*. Umbilical view. Zone E9, sample Sj.14. I: *Turborotalia frontosa*. Umbilical view. Zone E7b, sample Sj.11. J: *Globigerinatheka kugleri*. Spiral view. Zone E9, sample Sj.14. K: *Turborotalia frontosa*. Spiral view. Zone E9, sample Sj.14. L: *Hantkenina liebusi*. Spiral view. Zone E9, sample Sj.11. M: *Acarinina bullbrookii*. Spiral view. Zone E8, sample Sj.12. N: *Acarinina pentacamerata*. Spiral view. Zone E6, sample Sj.3. O: *Acarinina soldadoensis angulosa*. Spiral view. Zone E7b, sample Sj.11. P: *Hantkenina dumblei*. Spiral view. Zone E9, sample Sj.14. The scale bar is 100 µm.

to 21.03%; consequently, the K/S ratio increases to 5.92%. The illite content remains lower, with a trough of 2% at the base of the E9 Zone at sample Sj.14 (Table 2). Therefore, the peaks of kaolinite at the base and at the top of the section indicate increased

weathering rates and runoff on the adjacent continent, which in all likelihood were a consequence of increased precipitation and higher temperature and atmospheric CO₂ (Gaucher, 1981). The peaks could also be the result of progressively warmer and

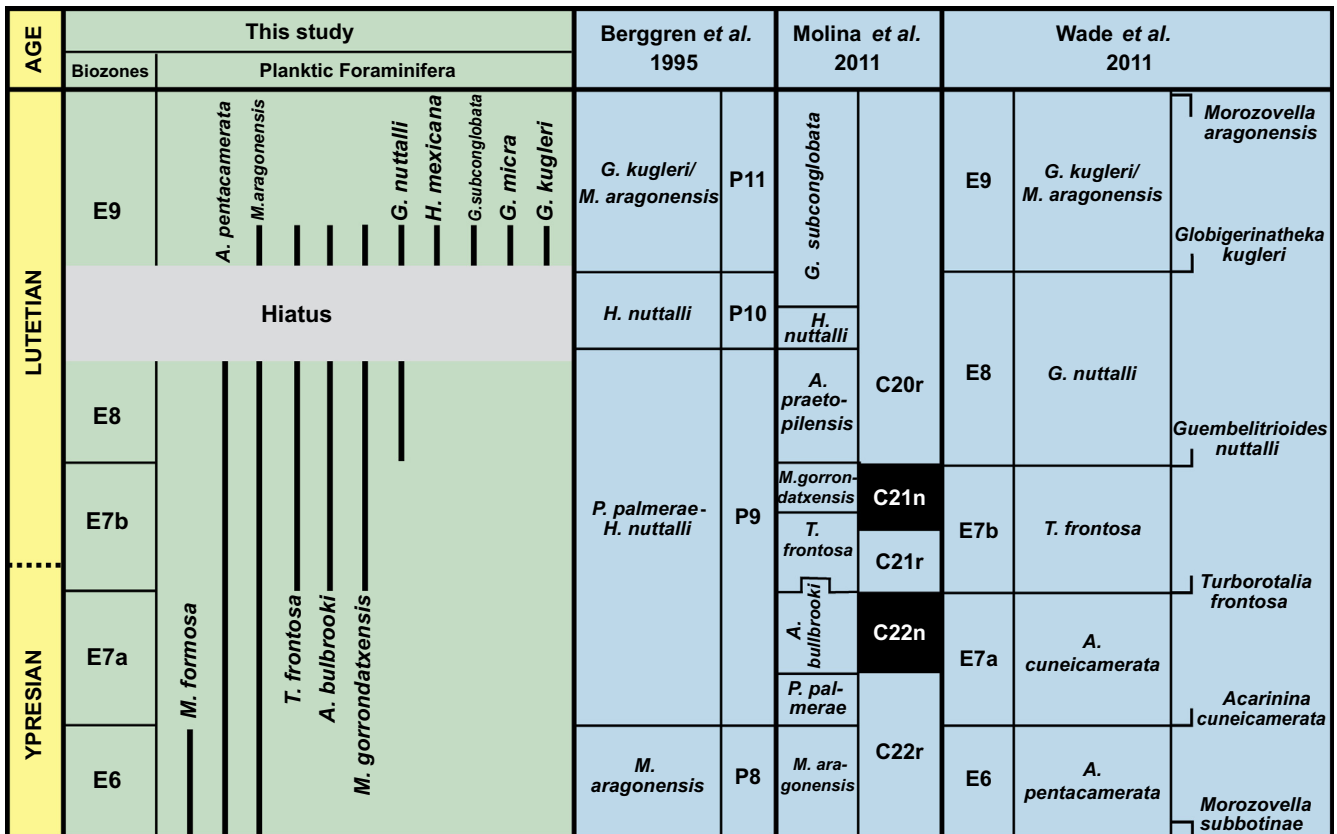


Fig. 6. Biozonation of the Y-L transition in the Sejnen section.

semi-arid climate with humidity, which fluctuated with warm seasons (Robert and Chamley, 1990, 1991; Robert and Kennett, 1992, 1994). These mineralogical variations suggest the climatic conditions: rather warm, tropical to subtropical and humid in northern Tunisia at the Y/L boundary. These warm conditions were probably inherited from the global warming that had already begun in the Paleocene/Eocene (Ortiz, 1995; Ben Ismail-Lattrache and Bobier, 1996; Karoui-Yaakoub, 1999, 2006; Thomas et al., 2000; Karoui-Yaakoub et al., 2011; Payros et al., 2012).

Regarding chemical elements, at the base of the E7b Zone (sample interval Sj.7-Sj.9), carbonate rates (CaO and CaCO₃) and SO₃ decrease and bottom out at the Sj.8 sample. In contrast, the contents of SiO₂, Al₂O₃, Fe₂O₃, MgO and K₂O increase with a large peak of silica (SiO₂) at the Sj.8 sample. The silica remains abundant throughout the section despite the variation of the contents, which indicates there the consistent presence of relatively coarse detrital materials (Fig. 5). These reflect very wet weather conditions at this time, with rainfall and mechanical alteration which increased in inland areas and were thus similar to many events in the Paleogene carbon cycle perturbation (Thiry, 2000; Schmitz et al., 2001; Schmitz and Pujalte, 2003, 2007; Nicolo et al., 2007; Agnini et al., 2009; Sluijs et al., 2009, 2011; Spofforth et al., 2010; Payros et al., 2012). This interval is considerably depleted in carbonate and enriched SiO₂, which is notable in the Gorrondatxe stratotype (Molina et al., 2011; Payros et al., 2012). Indeed, in this section, at the base of the Lutetian, there is an interval, at the transition from the Chron C21r/C21n, which is remarkable for its low carbonate content that interrupts the limestone-marl series (Fig. 5). In the interval Sj.11-Sj.14, corresponding to the top of the E7b, E8 and the base of E9 Zone, the rate of increase in carbonates and the decrease in the content of SiO₂, Al₂O₃ and K₂O indicate a limitation of detrital materials related to decreased rainfall, which would suggest a warming, sea level

rise and the limitation of detrital supplies. In summary, there are two intervals Sj.3-Sj.10 (the top of E6, E7a and the middle of E7b Zone) and Sj.11-Sj.14 (the top of E7b, E8 and the base of E9 Zone), during which two groups of compounds behave as antagonists: on the one hand, carbonates and SO₃ and on the other hand, detrital elements, namely: silica, alumina, K₂O, Fe₂O₃ and MgO.

6. Conclusions

The Sejnen section in northern Tunisia recorded during the Y/L boundary a series of events similar to those of the boundary stratotype defined at the Gorrondatxe section in northern Spain. All biozones across the Y/L boundary were recognized: E6, E7a, E7b, E8 and E9 Zones; however the limit E8/E9 is missing due to a hiatus. Below the Y/L boundary, planktic foraminifera were highly diversified with a predominance of tropical species of the genera *Morozovella* and *Acarinina*; these are indicators of warm waters compared to the cold-waters forms of the genus *Subbotina*, *Chiloguembelina* and *Pseudohastigerina*. In the Sejnen section, there is a drop in species richness of planktic foraminifera similar to that reported in the GSSP of Gorrondatxe precisely at the top of Chron C21r. At the top of the Sejnen section, planktic foraminifera again diversify and the cold seas forms with globular chambers begin to predominate slightly over the keeled forms of warm seas. This would suggest that the climate was rather warm at the Y/L boundary but then cooled somewhat at the lower Lutetian. A slight eustatic sea rise was also recorded above the Y/L boundary but the environment remained bathyal. Benthic foraminifera are very diversified and their association shows the coexistence of Velasco and Midway types and a major predominance of infaunal forms. An initial drop in the number of benthic foraminifera at the top of the E7b Zone was correlated with that reported at the Gorrondatxe section at the Chron C21n.

Therefore, by correlation with the stratotype of Gorrondatxe, the fall in benthic foraminifera of Sejnen section is located above the boundary Y/L. Just below the Y/L boundary, the calcareous tests of benthic foraminifera underwent a dissolution, whereas the number of benthic foraminifera with agglutinated tests reached a maximum and, therefore, the state of preservation of foraminifera becomes much deteriorated due to diagenesis.

The mineralogical results at the Sejnen section are also compared with those of the Gorrondatxe stratotype. At the Sejnen section, smectite is the most abundant mineral in the Y/L boundary, whereas the kaolinite dominates at the base of the Lutetian. In the section of Gorrondatxe, kaolinite is abundant in the whole interval. This comparison would indicate that in the Sejnen section at the Y/L boundary the climate was somewhat tropical to subtropical, the rainfall was lower and that an increase in sea level also probably occurred. The decrease in the number of benthic foraminifera in the middle and the top of the E7b Zone occurs at the same time as the maximum increase in the clay minerals content, especially smectite and illite. This would suggest a warming climate. Therefore, clay minerals, planktic and benthic foraminifera, indicate that at the Y-L interval, the environment was deep and bathyal with a warm climate. Geochemical results confirm once again the similarity between the two sections. Just below the Y/L boundary, the content of carbonates falls whereas the silica content increases. This drop in carbonate is very evident in the stratotype of Gorrondatxe and the abundance of silica and the compounds of Al_2O_3 , Fe_2O_3 , MgO and K_2O in Sejnen section. Likewise is evident in the same interval of the Gorrondatxe stratotype which is rich in turbidites.

In conclusion, at the Sejnen section, clay minerals, planktic and benthic foraminifera indicate that at the Y-L transition the environment was deep bathyal, stable, with low energy and warm with seasonal fluctuations. The Y-L transition at Gorrondatxe coincided with a maximum flooding that might be of eustatic origin and global in extension and we find the equivalent in the Sejnen section. Indeed, micropalaeontological, geochemical and mineralogical records allow us to conclude that the Y/L boundary occurs into the Sj.7-Sj.8 interval in a continuous marine sequence. Consequently, the Sejnen section is a suitable one across the Y/L boundary and is a potential auxiliary section or hypostratotype.

Acknowledgements

We would like to thank the research unit team Physique des Matériaux Lamellaires et Nanomatériaux Hybrides, the research unit team Pétrologie sédimentaire et cristalline of the Faculty of Sciences of Tunis, and the team of the Electronic Microscopy Scanning laboratory of the Tunisian Petroleum Development Company (ETAP). This study received financial support and assistance through Project CGL2011-23077 and Project CGL2014-58794P from the Spanish Ministry of Science and Technology (FEDER funds) and the Consolidated Group E05 from the Government of Aragón. We thank Dennis Delany (INTRATRAD) for correcting the English version of the text and two anonymous reviewers for their critical comments on an earlier draft, which have enhanced the final result.

References

- Agnini, C., Macrì, P., Backman, J., Brinkhuis, H., Fornaciari, E., Giusberti, L., Luciani, V., Rio, D., Sluijs, A., Speranza, F., 2009. An early Eocene carbon cycle perturbation at 52.5 Ma in the Southern Alps: chronology and biotic response. *Paleoceanography* 24, PA2209.
- Ali, J.R., Hailwood, E.A., 1995. Magnetostratigraphy of upper Paleocene through lower middle Eocene strata of NW Europe. In: Berggren, W.A., Kent, D.V., Aubry, P., Hardenbol, J. (Eds.), *Geochronology Time Scales and Global Stratigraphic Correlation*. SEPM Special Publication 54, pp. 275–279.
- Aubry, M.P., 1983. Biostratigraphie du Paléogène épicontinentale de l'Europe du Nord-Ouest. Étude fondée sur les nannofossiles calcaires. *Documents des Laboratoires de Géologie de Lyon* 89, 320 p.
- Aubry, M.P., 1986. Paleogene calcareous nanoplankton biostratigraphy of northwestern Europe. *Palaeogeogr. Palaeoclimatol. Palaeoecol.* 55 (2–4), 267–334.
- Bellier, J.P., Mathieu, R., Granier, B., 2010. Short Treatise on Foraminiferology (Essential on modern and fossil Foraminifera) [Court traité de foraminiférologie (L'essentiel sur les foraminifères actuels et fossiles)]. *Carnets de Géologie [Notebooks on Geology]*, Madrid, Book 2010/02 (CG2010_B02), 104 p. (10 Pls.).
- Ben Ayed, N., 1986. Évolution tectonique de l'avant-pays de la chaîne alpine de Tunisie du début du Mésozoïque à l'actuel. *Thèse de Doctorat ès Sciences*, Université Paris-Sud Orsay; Annales des Mines et de Géologie, Tunis 32, 286 p.
- Ben Ismail, K., 1994. Mise au point sur l'âge des formations Metlaoui et Souar en Tunisie. Notes du service Géologique de Tunisie, Tunis 60, pp. 59–87.
- Ben Ismail-Latrache, K., Bobier, C., 1996. Étude biostratigraphique, paléoécologique et paléobiogeographique des séries éocènes (Yprésien-Lutétien basal) de Tunisie centrale, in: *Géologie de l'Afrique et de l'Atlantique Sud*. Actes Colloque Angers 1994, pp. 563–583.
- Berggren, W.A., Aubert, J., 1975. Paleocene benthonic foraminiferal biostratigraphy and paleoecobiogeography of Atlantic Tethyan regions: midway-type fauna. *Palaeogeogr. Palaeoclimatol. Palaeoecol.* 18, 73–192.
- Berggren, W.A., Kent, D.V., Swisher, C.C., Aubry, M.A., 1995. A revised Paleogene geochronology and chronostratigraphy. In: Berggren, W.A., Kent, D.V., Aubry, P., Hardenbol, J. (Eds.), *Geochronology Time Scales and Global Stratigraphic Correlation*. SEPM Special Publication 54, pp. 129–212.
- Bernaola, G., Orue-Etxebarria, X., Payros, A., Dinarès-Turell, J., Tosquella, J., Apellaniz, E., Caballero, F., 2006. Biomagnetostratigraphic analysis of the Gorrondatxe section (Basque Country, Western Pyrenees): its significance for the definition of the Yprésien/Lutétien boundary stratotype. *Neues Jb. Geol. Paläontol. Abh.* 241, 67–109.
- Blondeau, A., 1981. Lutetian. In: Pomerol, C. (Ed.), *Stratotypes of Paleogene stages. Bulletin d'Information des Géologues du Bassin de Paris*, Mémoire hors série 2, pp. 167–180.
- Blow, W.H., 1979. The Cenozoic Globigerinida: a study of the morphology, taxonomy, evolutionary relationships and the stratigraphical distribution of some Globigerinida (mainly Globigerinacea), vol. 3. E.J. Brill, Leiden, 1413 p.
- Boscolo-Galazzo, F., Giusberti, L., Luciani, V., Thomas, E., 2013. Paleoenvironmental changes during the Middle Eocene Climatic Optimum (MECO) and its aftermath: the benthic foraminiferal record from the Alano section (NE Italy). *Palaeogeogr. Palaeoclimatol. Palaeoecol.* 378, 22–35.
- Chamley, H., 1971. Recherche sur la sédimentation argileuse en Méditerranée. *Sciences géologiques* 35, 180 p.
- Chamley, H., Deconinck, J.F., Millot, G., 1990. Sur l'abondance des minéraux smectitiques dans des périodes de haut niveau marin du Jurassique supérieur au Paléogène. *Comptes Rendus de l'Académie des Sciences, Paris, Serie II*, 311, pp. 1529–1536.
- Corliss, B.H., 1985. Microhabitats of benthic foraminifera within deep-sea sediments. *Nature* 314, 435–438.
- Corliss, B.H., Chen, C., 1988. Morphotype patterns of Norwegian Sea deep-sea benthic foraminifera and ecological implications. *Geology* 16, 716–719.
- El Ghali, A., Ben Ayed, N., Bobier, C.L., Zargouni, F., Krima, A., 2003. Les manifestations tectoniques synsédimentaires associées à la compression éocène en Tunisie: implications paléogéographiques et structurales sur la marge nord-africaine. *Comptes Rendus de Géosci.* 335 (9), 763–771.
- Gaucher, G., 1981. *Traité de pédologie agricole. Tome II: Les facteurs de la pédogenèse*. G. Lelotte Editions, Dison, 730 p.
- Gély, J.P., Sztrákos, K., 2000. L'évolution paléogéographique et géodynamique du Bassin aquitain au Paléogène: Enregistrement et datation de la tectonique pyrénéenne. *Géol. Fr. 2*, 31–57.
- Gonzalvo, C., Molina, E., 1998. Planktic foraminiferal biostratigraphy across the Lower-Middle Eocene transition in the Betic Cordillera (Spain). *Neues Jb. Geol. Paläontol. Abh.* 11, 671–693.
- Gonzalvo, C., Manchado, M.A., Molina, E., Rodríguez-Estrella, T., Romero, G., 2001. El límite Ypresiense/Luteciense en la Región de Murcia (Cordillera Bética, España). *Geogaceta* 29, 65–68.
- Holbourn, A., Henderson, A.S., Macleod, N., 2013. *Atlas of Benthic Foraminifera*. Wiley-Blackwell, 654 p.
- Hooyberghs, H.J.F., 1992. A new dating of the Brussels Sand Formation (Lower-Middle Eocene) on planktonic foraminifera from St-Stevens Woluwe and Neerijse, Belgium. *Tertiary Res.* 14, 33–49.
- Jamoussi, B., Bédir, M., Boukadi, N., Kharbachi, S., Zargouni, F., López-Galindo, A., Paquet, H., 2003. Répartition des minéraux argileux et contrôle tectono-eustatique dans les bassins de la marge tunisienne. *Comptes Rendus Géosci.* 335, 175–183.
- Jenkins, D.J., Luterbacher, H., 1992. Paleogene stages and their boundaries (Introductory remarks). *Neues Jb. Geol. Paläontol. Abh.* 186, 1–5.
- Jones, R.W., Charnock, M.A., 1985. "Morphogroups" of agglutinated foraminifera. Their life positions and feeding habits and potential applicability in (paleo)ecological studies. *Rev. Paléobiol.* 4, 311–320.
- Kaminski, M.A., Gradstein, F.M., 2005. *Atlas of Paleogene cosmopolitan deep-water agglutinated foraminifera*. Grzybowski Foundation. Special Publication 10, 547 p.
- Kaminski, M.A., Boersma, A., Tyszka, J., Holbourn, A.E.L., 1995. Response of deep-water agglutinated foraminifera to dysoxic conditions in the California Borderland Basins. In: Kaminski, M.A., Geroch, S., Gasinski, M.A., (Eds.),

- Proceedings of the Fourth International Workshop on Agglutinated Foraminifera, Kraków Poland, September 12–19, 1993. Grzybowski Foundation, Special Publication 3, pp. 131–140.
- Karoui-Yaakoub, N., 1999. Le Paléocène en Tunisie septentrionale et centro-orientale: Systématique, biostratigraphie des Foraminifères et environnement de dépôt. Ph D Thesis, Université de Tunis II, 357 p.
- Karoui-Yaakoub, N., 2006. Effet du réchauffement climatique global sur le comportement des foraminifères benthiques de l'intervalle de passage Paléocène-Eocène de la coupe d'Ellès (Tunisie). Rev. Paléobiol. 25, 575–591.
- Karoui-Yaakoub, N., Ben M'barek-Jemaï, M., Cherni, R., 2011. Le passage Paléocène-Eocène au nord de la Tunisie (Jebel Kharouba): Foraminifères planctoniques, minéralogie et environnement de dépôt. Rev. Paléobiol. 30, 105–121.
- Larrasoña, J.C., Gonzalvo, C., Molina, E., Monechi, S., Ortiz, S., Tori, F., Tosquella, J., 2008. Integrated magnetobiochronology of the Early/Middle Eocene transition at Agost (Spain): implications for defining the Ypresian/Lutetian boundary stratotype. Lethaia 41 (4), 395–415.
- Luterbacher, H.P., Ali, J.R., Brinkhuis, H., Gradstein, F.M., Hooker, J.J., Monechi, S., Ogg, J.G., Powell, J., Röhl, U., Sanfilippo, A., Schmitz, B., 2004. The Paleogene period. In: Gradstein, F.M., Ogg, J.G., Smith, A.G. (Eds.), A Geologic Time Scale 2004. Cambridge University Press, pp. 384–408.
- Martini, E., 1971. Standard Tertiary and Quaternary calcareous nannoplankton zonation. In: Farinacci, A., (Ed.), Proceedings of the Second Planktonic Conference Roma 1970. Edizioni Tecnoscienza, Roma 2, pp. 739–785.
- Molina, E., Cosovic, V., Gonzalvo, C., Von Salis, K., 2000. Integrated biostratigraphy across the Ypresian/Lutetian boundary at Agost, Spain. Revue de Micropaléontologie 43 (3), 1–19.
- Molina, E., Gonzalvo, C., Mancheño, M.A., Ortiz, S., Schmitz, B., Thomas, E., von Salis, K., 2006. Integrated stratigraphy and chronostratigraphy across the Ypresian-Lutetian transition in the Fortuna Section (Betic Cordillera, Spain). Newslett. Stratigr. 42 (1), 381–391.
- Molina, E., Alegret, L., Apellaniz, E., Bernaola, G., Caballero, F., Dinarès-Turell, J., Hardenbol, J., Heilmann-Clausen, C., Larrasoña, J.C., Luterbacher, H., Monechi, S., Ortiz, S., Orue-Etxebarria, X., Payros, A., Pujalte, V., Rodríguez-Tovar, F.J., Tori, F., Tosquella, J., Uchman, A., 2011. The Global Standard Stratotype-section and Point (GSSP) for the base of the Lutetian Stage at the Gorrondatxe section, Spain. Episodes 34 (2), 86–108.
- Nicol, M.J., Dickens, G.R., Hollis, C.J., Zachos, J.C., 2007. Multiple early Eocene hyperthermals: their sedimentary expression on the New Zealand continental margin and in the deep sea. Geology 35 (8), 699–702.
- Okada, H., Bukry, D., 1980. Supplementary modification and introduction of code numbers to the low-latitude coccolith biostratigraphic zonation (Bukry, 1973; 1975). Mar. Micropaleontol. 5, 321–325.
- Ortiz, N., 1995. Differential patterns of benthic foraminiferal extinctions near the Paleocene/Eocene boundary in the North Atlantic and the western Tethys. Mar. Micropaleontol. 26 (1–4), 341–359.
- Ortiz, N., Thomas, E., 2006. Lower-middle Eocene benthic foraminifera from the Fortuna Section (Betic Cordillera, southeastern Spain). Micropaleontology 52 (2), 97–150.
- Ortiz, S., Gonzalvo, C., Molina, E., Rodríguez-Tovar, F.J., Uchman, A., Vandenberghe, N., Zeelmakers, E., 2008. Palaeoenvironmental turnover across the Ypresian-Lutetian transition at the Agost section, southeastern Spain: in search of a marker event to define the Stratotype for the base of the Lutetian Stage. Mar. Micropaleontol. 69 (3–4), 297–313.
- Ortiz, S., Alegret, L., Payros, A., Orue-Etxebarria, X., Apellaniz, E., Molina, E., 2011. Distribution patterns of benthic foraminifera across the Ypresian-Lutetian Gorrondatxe section, Northern Spain: response to sedimentary disturbance. Mar. Micropaleontol. 78 (1–2), 1–13.
- Orue-Etxebarria, X., Payros, A., Bernaola, G., Dinares-Turell, J., Tosquella, J., Apellaniz, E., Caballero, F., 2006. The Ypresian/Lutetian boundary at the Gorrondatxe beach section (Basque Country, W Pyrenees). Climate and Biota of the Early Paleogene, Field Excursion Guidebook, Bilbao, 33 p.
- Orue-Etxebarria, X., Payros, A., Caballero, F., Molina, E., Apellaniz, E., Bernaola, G., 2009. The Ypresian/Lutetian transition in the Gorrondatxe beach (Getxo, western Pyrenees): review, recent advances and future prospects. Compilation and Abstract Book of the International Workshop on the Ypresian/Lutetian Boundary Stratotype (Getxo, 25–27 September 2009), University of the Basque Country, 215 pp.
- Payros, A., Orue-Etxebarria, X., Pujalte, V., 2006. Covaring sedimentary and biotic fluctuations in the Lower-Middle Eocene Pyrenean deep-sea deposits: palaeoenvironmental implications. Palaeogeogr. Palaeoclimatol. Palaeoecol. 234, 258–276.
- Payros, A., Bernaola, G., Orue-Etxebarria, X., Dinares-Turell, J., Tosquella, J., Apellaniz, E., 2007. Reassessment of the Early-Middle Eocene biomagnetochronology based on evidence from the Gorrondatxe section (Basque Country, western Pyrenees). Lethaia 40 (2), 183–195.
- Payros, A., Orue-Etxebarria, X., Bernaola, G., Apellaniz, E., Dinarès-Turell, J., Tosquella, J., Caballero, F., 2009a. Characterization and astronomically calibrated age of the first occurrence of *Turborotalia frontosa* in the Gorrondatxe section, a prospective Lutetian GSSP: implications for the Eocene time scale. Lethaia 42 (3), 255–264.
- Payros, A., Tosquella, J., Bernaola, G., Dinarès-Turell, J., Orue-Etxebarria, X., Pujalte, V., 2009b. Filling the North European Early/Middle Eocene (Ypresian/Lutetian) boundary gap: insights from the Pyrenean continental to deep-marine record. Palaeogeogr. Palaeoclimatol. Palaeoecol. 280 (3–4), 313–332.
- Payros, A., Ortiz, S., Alegret, L., Orue-Etxebarria, X., Apellaniz, E., Molina, E., 2012. An early Lutetian carbon-cycle perturbation: insights from the Gorrondatxe section (western Pyrenees, Bay of Biscay). Paleoceanography 27 (2), PA2213.
- Pearson, P.N., Olsson, R.K., Huber, B.T., Hemleben, C., Berggren, W.A. (Eds.), 2006. Atlas of Eocene Planktonic Foraminifera. Cushman Foundation for Foraminiferal Research, Special Publication 51, pp. 1–513.
- Robert, C., Chamley, H., 1990. Paleoenvironmental significance of clay-mineral associations at the Cretaceous-Tertiary passage. Palaeogeogr. Palaeoclimatol. Palaeoecol. 79 (3–4), 205–219.
- Robert, C., Chamley, H., 1991. Development of early Eocene warm climates, as inferred from clay-mineral variations in oceanic sediments. Palaeogeogr. Palaeoclimatol. Palaeoecol. 89 (4), 315–331.
- Robert, C., Kennett, J.P., 1992. Paleocene and Eocene kaolinite distribution in the south Atlantic and Southern Ocean: antarctic climatic and paleoceanographic implications. Mar. Geol. 103 (1–3), 99–110.
- Robert, C., Kennett, J.P., 1994. Antarctic subtropical humid episode at the Paleocene-Eocene boundary: clay-mineral evidence. Geology 22 (3), 211–214.
- Rodríguez-Tovar, F.J., Uchmann, A., Payros, A., Orue-Etxebarria, X., Apellaniz, E., Molina, E., 2010. Sea-level dynamic and palaecological factors affect in trace fossil distribution in Eocene turbiditic deposits from the Gorrondatxe section, N Spain. Palaeogeogr. Palaeoclimatol. Palaeoecol. 285, 50–65.
- Salaj, J., 1980. Microbiotriatigraphie du Crétacé et du Paléogène de la Tunisie septentrionale et orientale (hypostratotypes Tunisiens). Ph D Thesis, Institut géologique de Dionýz Stúr, Bratislava, 238 p. (64 Pls.).
- Schmitz, B., Pujalte, V., 2003. Sea-level, humidity, and land-erosion records across the initial Eocene thermal maximum from a continental-marine transect in northern Spain. Geology 31 (8), 689–692.
- Schmitz, B., Pujalte, V., 2007. Abrupt increase in seasonal extreme precipitation at the Paleocene-Eocene boundary. Geology 35 (3), 215–218.
- Schmitz, B., Pujalte, V., Nuñez-Betelu, K., 2001. Climate and sea-level perturbations during the Incipient Eocene Thermal Maximum: evidence from siliciclastic units in the Basque Basin (Ermaua, Zumaia and Trabakua Pass), northern Spain. Palaeogeogr. Palaeoclimatol. Palaeoecol. 165 (3–4), 299–320.
- Sluijs, A., Schouten, S., Donders, T.H., Schoon, P.L., Röhl, U., Reichart, G.J., Sangiorgi, F., Kim, J.H., Sanninge Damsté, J.S., Brinkhuis, H., 2009. Warm and wet conditions in the Arctic region during Eocene Thermal Maximum 2. Nat. Geosci. 2, 777–780.
- Sluijs, A., Bijl, P.K., Schouten, S., Röhl, U., Reichart, G.J., Brinkhuis, H., 2011. Southern ocean warming, sea level and hydrological change during the Paleocene-Eocene thermal maximum. Climate of the Past 7, 47–61.
- Speijer, R.P., 1994. Extinction and recovery patterns in benthic foraminiferal paleocommunities across the Cretaceous/Paleogene and Paleocene/Eocene boundaries. Geologica ultraiectina 124, 191 p.
- Spofforth, D.J.A., Agnini, C., Pälike, H., Rio, D., Fornaciari, E., Giusberti, L., Luciani, V., Lanci, L., Muttoni, G., 2010. Organic carbon burial following the middle Eocene climatic optimum in the central western Tethys. Paleoceanography 25 (3), PA3210.
- Stassen, P., Thomas, E., Speijer, R.P., 2012. Restructuring outer neritic foraminiferal assemblages in the aftermath of the Paleocene-Eocene thermal maximum. J. Micropaleontol. 31, 89–93.
- Steurbaut, É., 1988. New Early and Middle Eocene calcareous-nannoplankton events and correlation in middle to high latitudes of the northern hemisphere. Newslett. Stratigr. 18 (2), 99–115.
- Steurbaut, É., 2006. Ypresian. Geol. Belgica 9, 73–93.
- Thiry, M., 2000. Palaeoclimatic interpretation of clay minerals in marine deposits: an outlook from the continental origin. Earth-Sci. Rev. 49, 201–221.
- Thomas, E., Zachos, J.C., Bralower, T.J., 2000. Deep-sea environments on a Warm Earth: latest Paleocene-early Eocene. In: Huber, B.T., MacLeod, K.G., Wing, S.L. (Eds.), Warm climates in Earth history. Cambridge University Press, pp. 132–160.
- Toumarkine, M., Luterbacher, H.P., 1985. Paleocene and Eocene planktic foraminifera. In: Bolli, H.H., Saunders, J.B., Perch-Nielsen, K. (Eds.), Plankton Stratigraphy. Cambridge University Press, pp. 87–154.
- Valchev, B., 2007. Midway-type benthic foraminifera from the Paleocene of the coastal part of east staraplanina (Eastern Bulgaria). Family Textulariidae Ehrenberg, 1838 to family Stilostomellidae Finlay, 1947. Annual of the University Mining and Geology "ST. Ivan Rilski", Sofia, vol. 50, part I, (Geology and Geophysics), pp. 115–122.
- Vandenbergh, N., Laga, P., Steurbaut, É., Hardenbol, J., Vail, P.R., 1998. Tertiary Sequence Stratigraphy at the Southern Border of the North Sea Basin in Belgium. SEPM Special Publication 60, pp. 119–154.
- Vandenbergh, N., Hilgen, F., Speijer, R., Ogg, J.G., Gradstein, J.G., Hammer, F.M., Hollis, O., Hooker, J.J., 2012. The paleogene period. In: Gradstein, F., Ogg, J.G., Schmitz, M.D., Ogg, G.M. (Eds.), The Geologic Time Scale. Elsevier B.V., pp. 855–921.
- Wade, B.S., Pearson, P.N., Berggren, W.A., Pälike, H., 2011. Review and revision of Cenozoic tropical planktonic foraminiferal biostratigraphy and calibration to the geomagnetic polarity and astronomical time scale. Earth-Sci. Rev. 104, 111–142.